



Since January 2020 Elsevier has created a COVID-19 resource centre with free information in English and Mandarin on the novel coronavirus COVID-19. The COVID-19 resource centre is hosted on Elsevier Connect, the company's public news and information website.

Elsevier hereby grants permission to make all its COVID-19-related research that is available on the COVID-19 resource centre - including this research content - immediately available in PubMed Central and other publicly funded repositories, such as the WHO COVID database with rights for unrestricted research re-use and analyses in any form or by any means with acknowledgement of the original source. These permissions are granted for free by Elsevier for as long as the COVID-19 resource centre remains active.



Isothermal gene amplification coupled MALDI-TOF MS for SARS-CoV-2 detection

Guobin Han^a, Qiuyuan Lin^a, Jia Yi^a, Qian Lyu^b, Qingwei Ma^b, Liang Qiao^{a,*}

^a Department of Chemistry, Shanghai Stomatological Hospital, Fudan University, Shanghai, 200000, China

^b Bioyong Technologies, Inc., Beijing, 100176, China

ARTICLE INFO

Keywords:

SARS-CoV-2
Rolling circle amplification
MALDI-TOF MS
Gene detection
Virus analysis

ABSTRACT

The severe acute respiratory syndrome coronavirus 2 (SARS-CoV-2) has been spreading worldwide for more than a year and has undergone several mutations and evolutions. Due to the lack of effective therapeutics and long-active vaccines, accurate and large-scale screening and early diagnosis of infected individuals are crucial to control the pandemic. Nevertheless, the current widely used RT-qPCR-based methods suffer from complicated temperature control, long processing time and the risk of false-negative results. Herein, we present a three-way junction induced exponential rolling circle amplification (3WJ-eRCA) combined MALDI-TOF MS assay for SARS-CoV-2 detection. The assay can detect simultaneously the target nucleocapsid (N) and open reading frame 1 ab (orf1ab) genes of SARS-CoV-2 in a single test within 30 min, with an isothermal process (55 °C). High specificity to discriminate SARS-CoV-2 from other coronaviruses, like SARS-CoV, MERS-CoV and bat SARS-like coronavirus (bat-SL-CoVZC45), was observed. We have further used the method to detect pseudovirus of SARS-CoV-2 in various matrices, e.g. water, saliva and urine. The results demonstrated a great potential of the method for large scale screening of COVID-19, which is an important part of the pandemic control.

1. Introduction

Currently, the coronavirus disease 2019 (COVID-19) pandemic, which has resulted in devastating social and economic repercussions, still continues to spread throughout the world [1]. The disease is induced by severe acute respiratory syndrome coronavirus 2 (SARS-CoV-2) [2], which is an enveloped positive-sense single-stranded RNA (+ssRNA) virus, carrying one of the largest RNA genomes among all RNA virus families, i.e. nearly 30 kilobases [3]. Because there is a lack of effective therapeutics and long-active vaccines for COVID-19, the most effective approach to control the pandemic is till to practice social distancing and to screen symptomatic and asymptomatic infected individuals as fast as possible [4,5].

At present, the diagnosis of COVID-19 is mainly by serological test and nucleic acid test in terms of different biosensors [6]. Serological test is based on the detection of two specific antibodies, IgM and IgG, in patients' serum in response to the SARS-CoV-2 infection [7,8], which has the advantages of point-of-care testing, simple operation and low cost [9,10]. However, because of the delay in the generation of antibodies after SARS-CoV-2 infection, serological test can hardly be used for early diagnosis of COVID-19 [11,12]. The nucleic acid test directly

detecting SARS-CoV-2 viral RNA is regarded as a more suitable method for early, rapid and sensitive diagnosis of SARS-CoV-2 infection [13]. The reverse transcription-real time quantitative polymerase chain reaction (RT-qPCR) assay is globally utilized as the 'golden standard' for SARS-CoV-2 RNA detection due to its high sensitivity and specificity [13,14]. RT-qPCR assay performs reverse transcription reaction to convert the viral RNA into complementary DNA (cDNA), exponentially amplifies the cDNA, and finally detects the amplified DNA with fluorescence probes, which requires sophisticated operation and long turn-around time.

Since the outbreak of COVID-19, a series of novel methods based on viral RNA tests have been developed to detect SARS-CoV-2, including loop-mediated isothermal amplification (LAMP), reverse-transcription recombinase-aided amplification (RT-RAA), clustered regularly interspaced short palindromic repeats (CRISPR)-based diagnostics, microarray-based methods, etc. [15–18]. All the strategies are performed under constant temperature to achieve isothermal nucleic acid amplification, which provides simplified operations and lower costs for SARS-CoV-2 screening compared to RT-qPCR.

Matrix-assisted laser desorption/ionization time-of-flight mass spectrometry (MALDI-TOF MS) has been widely applied to the detection

* Corresponding author. Department of Chemistry, Fudan University, No 2005 Songhu Road, Shanghai, 200438, China.

E-mail address: liang.qiao@fudan.edu.cn (L. Qiao).

Table 1
Oligonucleotide sequences used in this work.

Nucleic acid note	Sequence (from 5' to 3')
N gene	CTGGCAATGGCGGTGATGCTGCTCTGTCTTGTCTGCTGCTGACAGATTG
N gene 3WJ-primer	AAGCAGCAGCAAAGCAACTGATTATG
N gene 3WJ-template	CAGACTCACACTGGTTGAGCTTTTGAAGAGCCATAATCGCAGCATCACCCGCCATTGCCAGTTTTT-p
N gene RC-template	p-TGAAGAGCTCTCACCTTGAGCATAACAGACTCACACTGGTTGAGCTACAGACTCACACTGGTTGAGC
orf1ab gene	GGGCTTTTGACATCTACAATGATAAAGTAGCTGGTTTTGCTAAATTCCTA
orf1ab gene 3WJ-primer	AGCAAACCAGCTACTTATCAATACT
orf1ab gene 3WJ-template	GCGACTCGTGGATGCACATATTTTGAAGAGCAGTATTGTCATTGTAGATGTCAAAGCCCCCCC-p
orf1ab gene RC-template	p-TGAAGAGCGCACCTACTAGTAGAAGCGACTCGTGGATGCACATAAAGCGACTCGTGGATGCACATA

of a number of biomolecules, and is well-known for its versatility, rapidity, and ease of implementation. The technique has recently brought revolutionary applications to the field of clinical diagnosis [19, 20]. For example, MALDI Biotyper (Bruker Daltonics) and VITEK MS (Biomérieux, Marcy l'Etoile) based on the principle of MALDI-TOF MS are the most widely used bacterial identification systems in clinical laboratories. They could achieve quick and reliable species identification by comparing a profile spectrum acquired from a microorganism to the corresponding profile signatures stored in a reference library [21]. On gene analysis, the MassARRAY (Agena Bioscience) platform based on PCR and MALDI-TOF MS has been used in various genetics and epigenetics research, and in clinical diagnosis of genetic disorders, including the quantitative analysis of gene expression, analysis of gene copy number variation (CNV), single nucleotide polymorphism (SNP) genotyping, DNA methylation identification, etc. [22–26].

Due to the superiority of high specificity and sensitivity of PCR and high throughput, high accuracy and flexibility of MALDI-TOF MS, PCR-MALDI-TOF MS has been developed as an alternative method for the detection of SARS-CoV-2 [27,28]. The PCR-MALDI-TOF MS-based assay exhibits higher specificity in the detection of SARS-CoV-2 than RT-qPCR [28]. Moreover, MALDI-TOF MS possesses the advantage of label-free and simultaneous detection of multi-mutations of SARS-CoV-2, which is not available in RT-qPCR [29]. However, the PCR-MALDI-TOF MS-based detection method needs bidirectional temperature control for multiple denaturation, annealing and extension in the PCR step, which makes the entire amplification detection time long [15,30]. Isothermal amplification of nucleic acids is a simple and efficient process that rapidly accumulates nucleic acid products at a constant temperature, which simplifies the operation compared to PCR [31].

Herein, we report a three-way junction induced exponential rolling circle amplification (3WJ-eRCA) combined MALDI-TOF MS for the detection of SARS-CoV-2 RNA. The method has the advantage of rapidity, high specificity and high throughput, and can simultaneously detect multiple genes for SARS-CoV-2 identification. High specificity to discriminate SARS-CoV-2 from other coronaviruses, like SARS-CoV, MERS-CoV and bat SARS-like coronavirus (bat-SL-CoVZC45), was achieved. We have further used the method to detect pseudovirus of SARS-CoV-2 from various matrices, e.g. water, saliva and urine. This method is also promising to be applied to large-scale epidemiological studies of different viruses as an effective supplement to the existing methods.

2. Experimental section

2.1. Reagents and materials

All HPLC-purified DNA oligonucleotides and pseudovirus of SARS-CoV-2 were synthesized by Sangon Biotech Co., Ltd. (Shanghai, China). The nicking endonucleases (Nt.BstNBI and Nt.BspQI) and the Vent (exo-) DNA polymerase were obtained from New England Biolabs (Beverly, MA). The dNTP mixture (dNTPs) and RNase-free water were purchased from TaKaRa Biotechnology Co., Ltd. (Dalian, China). The sequences of the oligonucleotides used in this work are listed in Table 1. Adsorbent resins were obtained from Bioyong Technology Co., Ltd. (Beijing, China).

2.2. SARS-CoV-2 gene isothermal amplification

The 3WJ-primer, 3WJ-template, and rolling circle probe were designed according to the partial sequence of nucleocapsid (N) gene and open reading frame 1 ab (orf1ab) gene of the SARS-CoV-2 (NCBI Reference Sequence: NC_045512.2). The online UNAFold web server (<http://www.unafold.org/>) was used to analyze the potential of oligonucleotide dimers and hairpins.

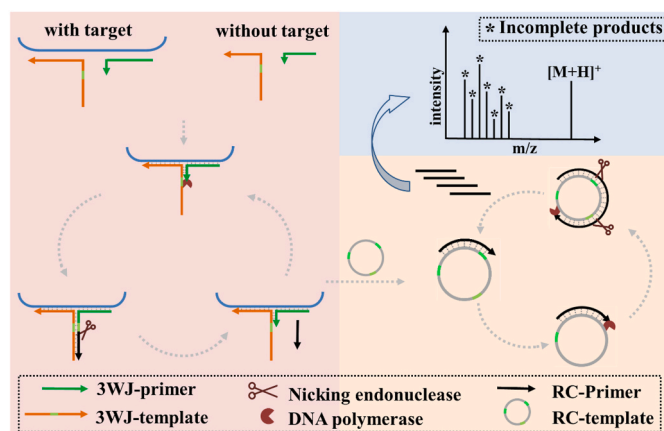
The reaction mixtures were separately prepared as solution A and solution B. Solution A was composed of 3WJ-template (10 nM), 3WJ-primer (10 nM), rolling circle probe (100 nM), dNTPs (750 μM), 0.5 × NEBuffer (25 mM Tris-HCl, pH 7.9, 50 mM NaCl, 5 mM MgCl₂, 50 μg/mL BSA) and different concentrations of target. The target was added to solution A and denatured at 90 °C for 5 min, then cooled to room temperature slowly to ensure the formation of the three-way junction complex structure. Solution B was composed of 1 U of Vent (exo-) DNA polymerase, 2 U of Nt.BstNBI, 2 U of Nt.BspQI, 1 × ThermoPol reaction buffer (20 mM Tris-HCl, pH 8.8, 10 mM KCl, 10 mM (NH₄)₂SO₄, 2 mM MgSO₄, 0.1% Triton X-100), and RNase-free water. 4 μL solution B was added to 6 μL solution A, and incubated at 55 °C to carry out the isothermal amplification. Triplicate experiments were performed for each condition to confirm the reproducibility of results.

2.3. RNA extraction from pseudovirus of SARS-CoV-2 and samples spiked with pseudovirus

The pseudovirus of SARS-CoV-2 contained the partial sequence of the orf1ab gene (13237–13737) and the full-length N gene of SARS-CoV-2 (NCBI Reference Sequence: NC_045512.2). The pseudovirus of SARS-CoV-2 (1 mL, 10⁸ copies/mL) was added into pre-centrifuged water, saliva, or urine (3 mL), respectively, to form the pseudovirus spiked samples. The nucleic acids of the pseudovirus were extracted and purified using the EZ-10 Spin Column Viral Total RNA Extraction Kit (Sangon Biotech (Shanghai) Co., Ltd.) by following the manufacturer's instructions, and finally collected in 30 μL of diethylpyrocarbonate (DEPC)-treated water. The collected samples were measured by SMA4000 UV-Vis Spectrophotometer (Meriton Ltd., Beijing, China) to determine the concentration of extracted RNA, and used immediately or stored at −80 °C for further usage. 1 μL of the extracted sample was added into solution A to perform the isothermal amplification, using the protocol as above mentioned.

2.4. Sample preparation and MALDI-TOF MS analysis

After the isothermal amplification, 10 μL of dispersed adsorbent resin (500 mg/mL) was added to the reaction mixture and incubated for 10 min under vortexing to remove salts. Then 0.5 μL of the purified product was deposited on a matrix pre-deposited microarray-chip plate (Bioyong Technology Co., Ltd., Beijing, China), and dried under ambient condition for MS analysis. The MALDI-TOF MS analysis was performed on a Clin-TOF II instrument (Bioyong Tech., China) under linear positive mode with the optimal parameters: laser frequency, 40 Hz; acceleration voltage, 20 kV; pulsed voltage, −2.1 kV; lens voltage, 6 kV; linear detector voltage, 2.8 kV; enable blanking mass, 1000 m/z; 300 laser shots;



Scheme 1. Schematic illustration of the three-way junction induced exponential rolling circle amplification (3WJ-eRCA) combined MALDI-TOF MS assay for SARS-CoV-2.

mass range, m/z 2000–10,000. External calibration was performed using 5 oligonucleotides with molecular weights of 5437.6, 6094.0, 6670.4, 7352.8, and 8407.5 Da, and the mass accuracy was calibrated within 1000 ppm.

3. Results and discussion

3.1. Design and demonstration of the 3WJ-eRCA combined MALDI-TOF MS assay

The strategy for SARS-CoV-2 detection on the basis of 3WJ-eRCA combined MALDI-TOF MS assay is shown in [Scheme 1](#). The formation of the three-way junction structure is the key step in the generation of the amplification products for MALDI-TOF MS analysis. The 3WJ-template is designed to contain a rolling circle primer (RC-primer) sequence at 5'-end and a complementary sequence to the target sequence of SARS-CoV-2 at 3'-end, which are separated by the recognition site of the nicking endonuclease Nt.BspQI and a complementary sequence of part of the 3WJ-primer. There is a 7-base-long sequence at the 3'-end of the 3WJ-primer, which can hybridize with the 3WJ-template. The 5'-end of 3WJ-primer can target the SARS-CoV-2 RNA. In the absence of the target RNA of the SARS-CoV-2, due to the inadequate complementarity of the 3WJ-primer and the 3WJ-template, the junction structure cannot form stably. When the target RNA from SARS-CoV-2 exists, the 3WJ-primer and 3WJ-template can hybridize stably to form the three-way junction structure. Therefore, a large number of RC-primers as the trigger strands are generated after the repeated cycles of extension and cleavage of the 3WJ-primer by Vent (exo-) DNA polymerase and Nt.BspQI nicking endonuclease. In the next rolling circle amplification reaction, the rolling circle template (RC-template) is composed of a hybridization sequence to RC-primers and nicking site for Nt.BstNBI and Nt.BspQI nicking endonuclease. Once the RC-primer is generated and forms a complex with the RC-template, a cascade reaction of linear rolling circle amplification in the presence of Vent (exo-) polymerase can be initiated, synthesizing a long repeat complementary sequence of the RC-template. This amplified repeat sequence is then cut by Nt.BstNBI and Nt.BspQI nicking endonucleases, and multiple short new DNA products are produced, which serve as new triggers to further initiate new extension circles. Consequently, large numbers of products are obtained through the exponential amplification reaction for MALDI-TOF MS detection, achieving a highly sensitive assay for SARS-CoV-2.

To demonstrate the feasibility of the method, partial sequences of the orf1ab gene (from 13538 to 13587) and N gene (from 28905 to 28954) of SARS-CoV-2 were selected as target genes, because the RdRp region of orf1ab gene can differentiate SARS-CoV-2 from the SARS-CoV, and the N

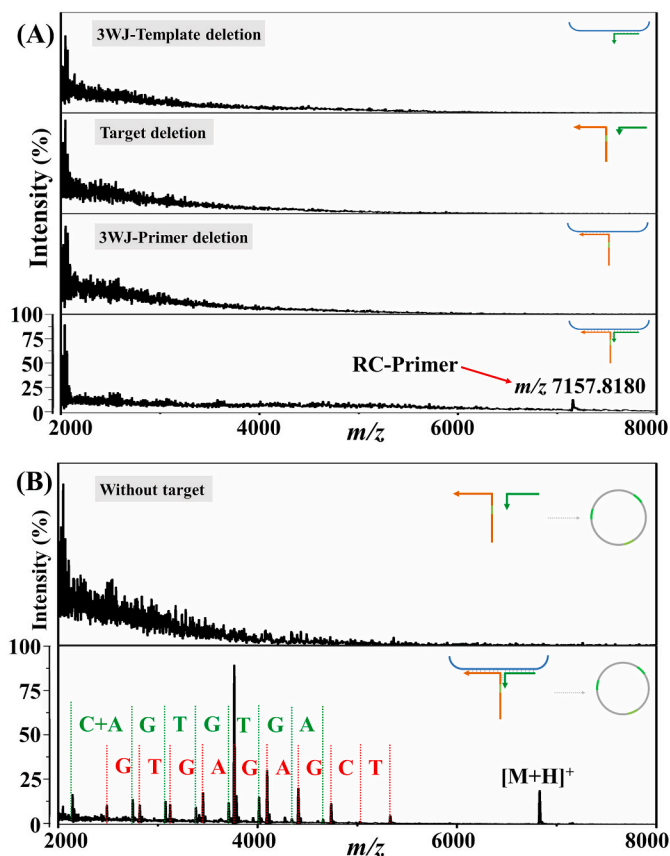


Fig. 1. 3WJ-eRCA combined MALDI-TOF MS assay for target N gene detection. (A) Component deletion experiments to confirm the formation of the three-way junction complex. (B) The target N gene detection. The concentration of target N gene was 10 nM. The detailed sequences and corresponding molecular weight values of the peaks are listed in [Table S1](#).

gene is conserved among all beta coronaviruses [2,32]. As shown in [Fig. 1A](#), in the presence of the target N gene, the expected peak signal of MALDI-TOF MS for N gene RC-primer can be observed. As a comparison, the peak signal was disappeared when any of the three-way junction structure components was absent. The whole experiment of the 3WJ-eRCA was performed in the absence or presence of the target N gene to further investigate the feasibility of the MALDI-TOF MS assay. It can be seen from [Fig. 1B](#) that there was no MS signal when the target N gene was absent. In the presence of the target N gene, the peaks from extended oligonucleotides were detected. After sequence alignment, the peak at $\sim m/z$ 7 k (labeled as $[M+H]^+$) is the final amplification product. A number of peaks between m/z 2000 and m/z 6000 are the incomplete extended sequences. The detailed sequences and corresponding molecular weight values of the peaks are listed in [Table S1](#). Similar results were observed with the orf1ab target gene, as shown in [Fig. S1](#) and [Table S2](#). It was observed that the signal intensity of the complete extension products was not the highest among all extension products, and was gradually weakened with the decrease of target gene concentration, and eventually disappeared. Nevertheless, both the final amplification products and the incomplete extended sequences are specific to the presence of target genes. Therefore, any of the peaks could be used for SARS-CoV-2 detection.

3.2. Performance of the 3WJ-eRCA combined MALDI-TOF MS assay

To achieve the optimal performance of the assay, the experimental conditions, including reaction temperature, the concentrations of

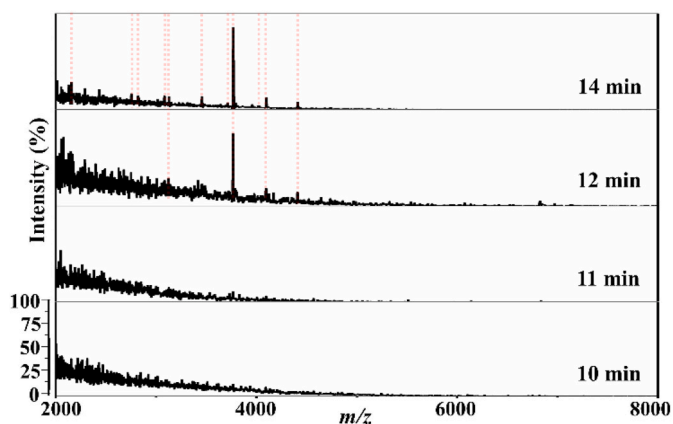


Fig. 2. The MALDI-TOF MS spectra of background amplification of the 3WJ-eRCA assay for the target N gene detection with varied reaction time. Red dashed line: extension products. (For interpretation of the references to colour in this figure legend, the reader is referred to the Web version of this article.)

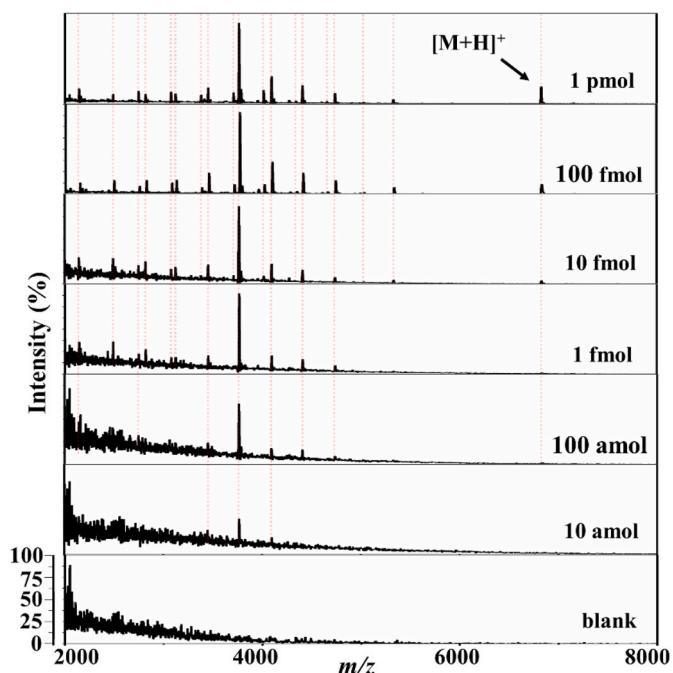


Fig. 3. The MALDI-TOF MS spectra of the 3WJ-eRCA assay triggered by different amounts of the target N gene in 10 μ L reaction mixture. Red dashed line: extension products. $[M+H]^+$: molecular ion of the complete extension product. (For interpretation of the references to colour in this figure legend, the reader is referred to the Web version of this article.)

polymerase, nicking endonuclease, 3WJ-primer, 3WJ-template and RC-template, were optimized. Real-time fluorescence measurements were performed on a LineGene 9640 real-time nucleic acids amplification system (Hangzhou Bioer Technology Co., Ltd. Hangzhou, China) to assess the optimal experimental conditions (data not shown). The final optimal conditions are: 55 $^{\circ}$ C reaction temperature; 1 U Vent (exo-) DNA polymerase; 4 U nicking endonuclease; 10 nM 3WJ-primer; 10 nM 3WJ-template and 100 nM RC-template.

The isothermal amplification normally suffers from background amplification. It was found that if the amplification reaction time was long enough, even in the absence of the target gene, a series of strong MS signals of the amplification products could still be detected. Therefore, the investigation of non-specificity amplification reaction time is crucial for the 3WJ-eRCA-MALDI-TOF MS assay. As shown in Fig. 2, when the

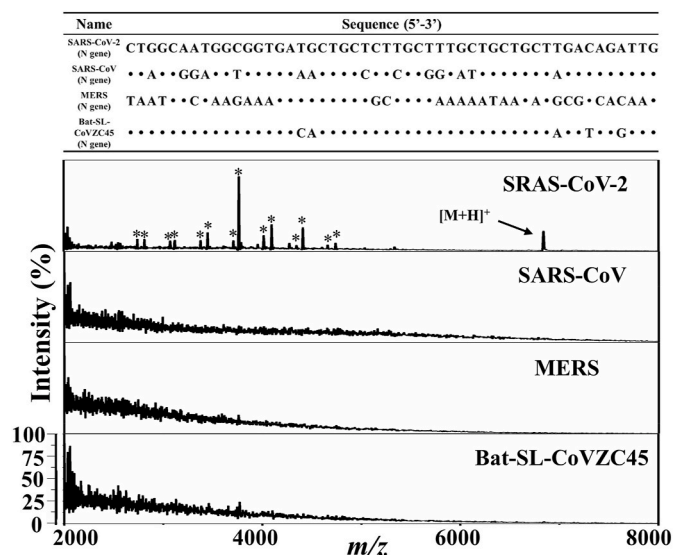


Fig. 4. The specificity of the 3WJ-eRCA assay combined MALDI-TOF MS for target N gene detection. Top panel: Comparison of target N gene sequences between SARS-CoV-2 (accession NC_045512.2), SARS-CoV (accession NC_004718.3), MERS (NC_019843.3), and bat-SL-CoVZC45 (accession MG772933.1). The matched bases are replaced with “□”. Lower panel: MALDI-TOF MS spectra of the 3WJ-eRCA assay triggered by 100 nM N gene fragments from different coronavirus as shown in top panel. *: incomplete extension products. $[M+H]^+$: molecular ion of the complete extension product.

amplification reaction time was longer than 11 min, the MS signal of extended oligonucleotides was observed even without the target gene. Hence, 11 min was selected as the optimal amplification time for the target N gene detection. It was found that 11 min was also the optimal amplification time for the target orf1ab gene detection (Fig. S2). Taken into consideration of the sample preparation steps, the total assay time was then less than 30 min for the analysis of extracted RNA samples.

Under the optimized experimental condition, the sensitivity of the 3WJ-eRCA-MALDI-TOF MS assay was evaluated using 10-fold serial dilutions of the target N gene ranging from 1 pmol/10 μ L to 10 amol/10 μ L. As shown in Fig. 3, with the increase of the amount of the target N gene, an increased MS signal was observed. The experimental results of the target orf1ab gene sensitivity investigation are presented in Fig. S3. The experimental results demonstrated that the method can detect both the target N gene and the target orf1ab gene of SARS-CoV-2 at a concentration as low as 10 amol/10 μ L (1 pM). Reproducibility of detecting the target N gene and the orf1ab gene at 1 pM was shown in Fig. S4 and S5. The day-to-day reproducibility of the analysis was also assessed with a 3-day interval (Fig. S4 and S5). A number of extension products can be repeatedly detected with 1 pM target gene in triplicate. All the results demonstrated a good reproducibility of the developed assay.

Since SARS-CoV, MERS-CoV, bat-SL-CoVZC45 and SARS-CoV-2 have a high similarity in genome [32], the specificity of the 3WJ-eRCA combined MALDI-TOF MS assay was assessed by considering the four coronaviruses. The target N gene of SARS-CoV-2 was aligned to the genome of the other three coronaviruses, and the corresponding gene sequences with highest similarity to the target N gene of SARS-CoV-2 are shown in Fig. 4. Under the optimized experimental condition, only in the presence of the target N gene of SARS-CoV-2, significant MS signal of amplification products was observed. The specificity of the method against the target orf1ab gene was assessed in a similar way. High specificity against the target orf1ab gene of SARS-CoV-2 was also observed (Fig. S6). Therefore, the developed assay can provide specific SARS-CoV-2 detection.

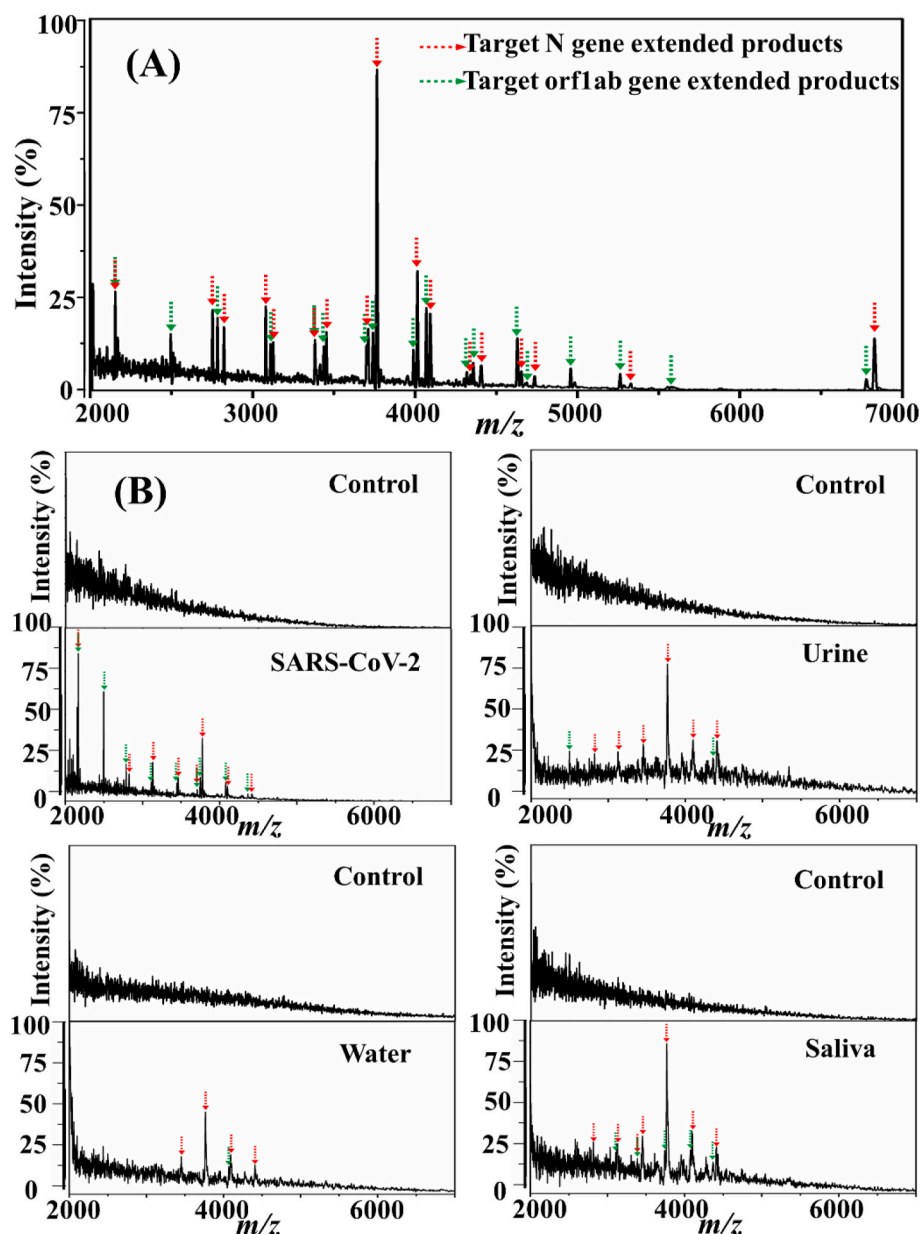


Fig. 5. (A) Simultaneous dual-gene detection by the 3WJ-eRCA coupled MALDI-TOF MS. The concentration of each target gene was 10 nM. (B) Detection of SARS-CoV-2 pseudovirus and the pseudovirus in complex samples. The concentration of extracted RNA was in the range of 2.0–4.8 ng/ μ L. The control was performed using the same matrix of each condition without pseudovirus. Red arrow: extension products from N gene; green arrow: extension products from orf1ab gene. (For interpretation of the references to colour in this figure legend, the reader is referred to the Web version of this article.)

3.3. Detection of dual-gene and SARS-CoV-2 pseudovirus by the 3WJ-eRCA combined MALDI-TOF MS assay

To further assess the analytical performance of the 3WJ-eRCA combined MALDI-TOF MS assay, the target N and orf1ab genes were detected simultaneously by adding the 3WJ-primer, 3WJ-template, and RC-template for both targets. The amplification reaction time and sensitivity were investigated for the simultaneous dual-gene detection. As shown in Fig. S7, compared to the single target gene detection, the reaction time of dual-gene nonspecific amplification was slightly delayed, and a weak background MS signal appeared at 13 min, indicating that the amplification reaction of 3WJ-eRCA can be terminated at 12 min for the dual-gene detection. Under the optimal reaction time, the method can simultaneously detect both target N and orf1ab gene of SARS-CoV-2 with the concentration as low as 10 amol/10 μ L (1 pM) each, Fig. S8. Fig. 5A shows the MS signal of the 3WJ-eRCA assay for the two target genes (10 nM each) simultaneously. The reproducibility of the dual-gene detection was also investigated and shown in Fig. S9. A number of extension products from the dual-gene amplification can be

repeatedly detected with 1 pM target gene in triplicate. These results demonstrated that the 3WJ-eRCA combined MALDI-TOF MS assay can realize dual-gene detection in a single test. Since mass spectrometry has a high resolving power and a high capacity of signals, even more gene fragments can be detected simultaneously when the corresponding 3WJ-reactants are designed and employed.

To demonstrate the performance of the 3WJ-eRCA combined MALDI-TOF MS assay in complex samples, the RNA extracted from pseudovirus of SARS-CoV-2, as well as water, saliva and urine samples spiked with pseudovirus of SARS-CoV-2 were analyzed. The concentration of the extracted RNA was in the range of 2.0–4.8 ng/ μ L measured by spectrophotometer. Blank control was performed for each sample by using the same matrix without the pseudovirus. As shown in Fig. 5B, the MALDI-TOF MS signal of extended products from N gene (red arrow) and orf1ab gene (green arrow) by 3WJ-eRCA could be obviously detected from the pseudovirus and pseudovirus spiked sample, distinguishing clearly from the blank control. However, the complete extension products were absent in all groups, maybe due to the low concentration of extracted target gene from the complex samples. All

these results demonstrated that the proposed method can be used to detect SARS-CoV-2 in complex matrices, indicating the potential application of the method in real case analysis.

Finally, the analytical performance of the method for COVID-19 detection was compared with other recently reported methods (Table S3). To date, the MS-based assays for COVID-19 detection include inductively coupled plasma mass spectrometry (ICP-MS)-based, MALDI-MS-based and liquid chromatography mass spectrometry (LC-MS)-based methods, targeting at the specific nucleic acids or proteins. The ICP-MS based method employed additional nanoparticle probes to detect the specific nucleic acids of SARS-CoV-2 [33,34]. LC-MS and high resolution MALDI-MS were used to detect virus proteins directly [35,36]. MALDI-MS were also combined with PCR to detect virus nucleic acids [27]. Compared to the MS-based assays, our method provides a comparable sensitivity while a simple and easy-to-operate experimental procedure. Compared to non-MS-based assay, where electrochemical signal, fluorescent signal, surface plasmon resonance signal, etc. were employed to report the presence of virus nucleic acid [37–42], the MS-based assays, including our method, normally suffer from lower sensitivity. However, MS can directly detect the target molecules or the amplification products of target molecules without any additional labelling methods, i.e. in a label-free manner, largely avoiding the false results arisen from background signal.

4. Conclusion

In summary, a three-way junction induced exponential rolling circle amplification (3WJ-eRCA) combined MALDI-TOF MS detection assay was established to detect the target N gene and orf1ab gene fragments of SARS-CoV-2. The assay can be performed in an isothermal process within 30 min, preventing the long turnaround time of temperature cycling. With the advantages of high throughput and high accuracy of MALDI-TOF MS analysis, it is possible to analyze multiple genes and even detect SARS-CoV-2 mutation by the method, greatly improving detection accuracy and efficiency. Meanwhile, the assay can discriminate SARS-CoV-2 from other closely related coronaviruses, e.g. SARS-CoV, MERS-CoV, and bat-SL-CoVZC45, showing high specificity. The successful identification of SARS-CoV-2 pseudovirus from complex matrices indicates the potential of the method in real application. With the principle of the 3WJ-eRCA and the MALDI-TOF MS, the method is not limited to the detection of SARS-CoV-2, but also many other nucleic acid-based biomarkers.

Credit author statement

Guobin Han: Conceptualization, Methodology, Investigation, Writing – original draft. Qiuyuan Lin: Review & Editing. Jia Yi: Review & Editing. Qian Lyu: Resources. Qingwei Ma: Resources. Liang Qiao: Conceptualization, Writing – review & editing, Supervision, Funding acquisition.

Declaration of competing interest

The authors declare that they have no known competing financial interests or personal relationships that could have appeared to influence the work reported in this paper.

Acknowledgements

This work was supported by the Ministry of Science and Technology of China (2020YFF0426500, 2020YFF0304502) and National Natural Science Foundation of China (NSFC, 22022401, 22074022 and 21934001).

Appendix A. Supplementary data

Supplementary data to this article can be found online at <https://doi.org/10.1016/j.talanta.2022.123297>.

References

- [1] E. Callaway, H. Ledford, G. Viglione, T. Watson, A. Witze, Covid and 2020, *Nature* 588 (2020) 550–552.
- [2] P. Zhou, X.L. Yang, X.G. Wang, B. Hu, L. Zhang, W. Zhang, H.R. Si, Y. Zhu, B. Li, C. L. Huang, H.D. Chen, J. Chen, Y. Luo, H. Guo, R.D. Jiang, M.Q. Liu, Y. Chen, X. R. Shen, X. Wang, X.S. Zheng, K. Zhao, Q.J. Chen, F. Deng, L.L. Liu, B. Yan, F. X. Zhan, Y.Y. Wang, G.F. Xiao, Z.L. Shi, A pneumonia outbreak associated with a new coronavirus of probable bat origin, *Nature* 579 (2020) 270–273.
- [3] R. Rangan, I.N. Zheludev, R.J. Hagey, E.A. Pham, H.K. Wayment-Steele, J.S. Glenn, R. Das, RNA genome conservation and secondary structure in SARS-CoV-2 and SARS-related viruses: a first look, *RNA* 26 (2020) 937–959.
- [4] S.M. Moghadas, M.C. Fitzpatrick, P. Sah, A. Pandey, A. Shoukat, B.H. Singer, A. P. Galvani, The implications of silent transmission for the control of COVID-19 outbreaks, *Proc. Natl. Acad. Sci. U.S.A.* 117 (2020) 17513–17515.
- [5] M. Salathe, C.L. Althaus, R. Neher, S. Stringhini, E. Hodcroft, J. Fellay, M. Zwahlen, G. Senti, M. Battegay, A. Wilder-Smith, I. Eckerle, M. Egger, N. Low, COVID-19 epidemic in Switzerland: on the importance of testing, contact tracing and isolation, *Swiss Med. Wkly.* 150 (2020), w20225.
- [6] M. Drobysh, A. Ramanaviciene, R. Viter, C.-F. Chen, U. Samukaite-Bubniene, V. Ratautaite, A. Ramanavicius, Biosensors for the determination of SARS-CoV-2 virus and diagnosis of COVID-19 infection, *Int. J. Mol. Sci.* 23 (2022), 666.
- [7] Q. Lin, D. Wen, J. Wu, L. Liu, W. Wu, X. Fang, J. Kong, Microfluidic immunoassays for sensitive and simultaneous detection of IgG/IgM/antigen of SARS-CoV-2 within 15 min, *Anal. Chem.* 92 (2020) 9454–9458.
- [8] M. Drobysh, A. Ramanaviciene, R. Viter, A. Ramanavicius, Affinity sensors for the diagnosis of COVID-19, *Micromachines* 12 (2021), 390.
- [9] C.Y. Lee, R.T.P. Lin, L. Renia, L.F.P. Ng, Serological approaches for COVID-19: epidemiologic perspective on surveillance and control, *Front. Immunol.* 11 (2020), 879.
- [10] F. Amanat, D. Stadlbauer, S. Strohmaier, T.H.O. Nguyen, V. Chromikova, M. McMahon, K. Jiang, G.A. Arunkumar, D. Jurczyszak, J. Polanco, M. Bermudez-Gonzalez, G. Kleiner, T. Aydllo, L. Miorin, D.S. Fierer, L.A. Lugo, E.M. Kojic, J. Stoeber, S.T.H. Liu, C. Cunningham-Rundles, P.L. Felgner, T. Moran, A. Garcia-Sastre, D. Caplivski, A.C. Cheng, K. Kedzierska, O. Vapalahti, J.M. Hepojoki, V. Simon, F. Krammer, A serological assay to detect SARS-CoV-2 seroconversion in humans, *Nat. Med.* 26 (2020) 1033–1036.
- [11] E. Xiong, L. Jiang, T. Tian, M. Hu, H. Yue, M. Huang, W. Lin, Y. Jiang, D. Zhu, X. Zhou, Simultaneous dual-gene diagnosis of SARS-CoV-2 based on CRISPR/Cas9-mediated lateral flow assay, *Angew. Chem. Int. Ed.* 60 (2021) 5307–5315.
- [12] J.P. Broughton, X. Deng, G. Yu, C.L. Fasching, V. Servellita, J. Singh, X. Miao, J. A. Streithorst, A. Granados, A. Sotomayor-Gonzalez, K. Zorn, A. Gopez, E. Hsu, W. Gu, S. Miller, C.Y. Pan, H. Guevara, D.A. Wadford, J.S. Chen, C.Y. Chiu, CRISPR-Cas12-based detection of SARS-CoV-2, *Nat. Biotechnol.* 38 (2020) 870–874.
- [13] M.N. Esbin, O.N. Whitney, S.S. Chong, A. Maurer, X. Darzacq, R. Tjian, Overcoming the bottleneck to widespread testing: a rapid review of nucleic acid testing approaches for COVID-19 detection, *RNA* 26 (2020) 771–783.
- [14] B. Udugama, P. Kadhiresan, H.N. Kozlowski, A. Malekjahani, M. Osborne, V.Y. C. Li, H.M. Chen, S. Mubareka, J.B. Gubbay, W.C.W. Chan, Diagnosing COVID-19: the disease and tools for detection, *ACS Nano* 14 (2020) 3822–3835.
- [15] B. Pang, J. Xu, Y. Liu, H. Peng, W. Feng, Y. Cao, J. Wu, H. Xiao, K. Pabbaraju, G. Tipples, M.A. Joyce, H.A. Saffran, D.L. Tyrrell, H. Zhang, X.C. Le, Isothermal amplification and ambient visualization in a single tube for the detection of SARS-CoV-2 using loop-mediated amplification and CRISPR technology, *Anal. Chem.* 92 (2020) 16204–16212.
- [16] G. Xue, S. Li, W. Zhang, B. Du, J. Cui, C. Yan, L. Huang, L. Chen, L. Zhao, Y. Sun, N. Li, H. Zhao, Y. Feng, Z. Wang, S. Liu, Q. Zhang, X. Xie, D. Liu, H. Yao, J. Yuan, Reverse-transcription recombinase-aided amplification assay for rapid detection of the 2019 novel coronavirus (SARS-CoV-2), *Anal. Chem.* 92 (2020) 9699–9705.
- [17] W. Feng, A.M. Newbigging, J. Tao, Y. Cao, H. Peng, C. Le, J. Wu, B. Pang, J. Li, D. L. Tyrrell, H. Zhang, X.C. Le, CRISPR technology incorporating amplification strategies: molecular assays for nucleic acids, proteins, and small molecules, *Chem. Sci.* 12 (2021) 4683–4698.
- [18] H. Xiong, X. Ye, Y. Li, J. Qi, X. Fang, J. Kong, Efficient microfluidic-based air sampling/monitoring platform for detection of aerosol SARS-CoV-2 on-site, *Anal. Chem.* 93 (2021) 4270–4276.
- [19] P. Seng, J.M. Rolain, P.E. Fournier, B. La Scola, M. Drancourt, D. Raoult, MALDI-TOF-mass spectrometry applications in clinical microbiology, *Future Microbiol.* 5 (2010) 1733–1754.
- [20] P. Lasch, D. Jacob, R. Grunow, T. Schwecke, J. Doellinger, Matrix-assisted laser desorption/ionization time-of-flight (MALDI-TOF) mass spectrometry (MS) for the identification of highly pathogenic bacteria, *Trends Anal. Chem.* 85 (2016) 103–111.
- [21] H. Wang, Y.Y. Fan, T. Kudinha, Z.P. Xu, M. Xiao, L. Zhang, X. Fan, F.R. Kong, Y. C. Xu, A comprehensive evaluation of the Bruker Biotyper MS and vitek MS matrix-assisted laser desorption ionization-time of flight mass spectrometry systems for identification of yeasts, part of the National China Hospital Invasive Fungal

- surveillance Net (CHIF-NET) study, 2012 to 2013, *J. Clin. Microbiol.* 54 (2016) 1376–1380.
- [22] M.B. Lambros, P.M. Wilkerson, R. Natrajan, N. Patani, V. Pawar, R. Vatcheva, M. Mansour, M. Laschet, B. Oelze, N. Orr, S. Muller, J.S. Reis-Filho, High-throughput detection of fusion genes in cancer using the Sequenom MassARRAY platform, *Lab. Invest.* 91 (2011) 1491–1501.
- [23] F. Xie, J. Huang, S. Qu, W. Wu, J. Jiang, H. Wang, S. Wang, Q. Liu, S. Zhang, L. Xu, S. Gao, Y. Zhang, J. Zhao, W. Chen, Sensitive detection of trace amounts of KRAS codon 12 mutations by a fast and novel one-step technique, *Clin. Biochem.* 47 (2014) 237–242.
- [24] Y. Belloum, M. Janning, M. Mohme, R. Simon, J. Kropidlowski, A. Sartori, D. Irwin, M. Westphal, K. Lamszus, S. Loges, S. Riethdorf, K. Pantel, H. Wikman, Discovery of targetable genetic alterations in NSCLC patients with different metastatic patterns using a MassARRAY-based circulating tumor DNA assay, *Cells* 9 (2020).
- [25] S. Sauer, R. Reinhardt, H. Lehrach, I.G. Gut, Single-nucleotide polymorphisms: analysis by mass spectrometry, *Nat. Protoc.* 1 (2006) 1761–1771.
- [26] R. Claus, S. Wilop, T. Hielscher, M. Sonnet, E. Dahl, O. Galm, E. Jost, C. Plass, A systematic comparison of quantitative high-resolution DNA methylation analysis and methylation-specific PCR, *Epigenetics* 7 (2012) 772–780.
- [27] M.M. Hernandez, R. Banu, P. Shrestha, A. Patel, F. Chen, L. Cao, S. Fabre, J. Tan, H. Lopez, N. Chiu, B. Shifrin, I. Zapolskaya, V. Flores, P.Y. Lee, S. Castaneda, J. D. Ramirez, J. Jhang, G. Osorio, M.R. Gitman, M.D. Nowak, D.L. Reich, C. Cordon-Cardo, E.M. Sordillo, A.E. Paniz-Mondolfi, RT-PCR/MALDI-TOF mass spectrometry-based detection of SARS-CoV-2 in saliva specimens, *J. Med. Virol.* 93 (2021) 5481–5486.
- [28] J. Wang, D. Zhang, Q.Q. Chen, J.L. Yu, Y. Yang, L. Qiao, Y. Sun, Establishment and application of PCR-Time-of-flight mass spectrometer for SARS-CoV-2 nucleic acid detection, *Chin. Gen. Pract.* 23 (2020) 4430–4435.
- [29] M. Rybicka, E. Milosz, K.P. Bielawski, Superiority of MALDI-TOF mass spectrometry over real-time PCR for SARS-CoV-2 RNA detection, *Viruses* 13 (2021), 730.
- [30] W. Feng, A.M. Newbigging, C. Le, B. Pang, H. Peng, Y. Cao, J. Wu, G. Abbas, J. Song, D.-B. Wang, M. Cui, J. Tao, D.L. Tyrrell, X.-E. Zhang, H. Zhang, X.C. Le, Molecular diagnosis of COVID-19: challenges and research needs, *Anal. Chem.* 92 (2020) 10196–10209.
- [31] Y. Zhao, F. Chen, Q. Li, L. Wang, C. Fan, Isothermal amplification of nucleic acids, *Chem. Rev.* 115 (2015) 12491–12545.
- [32] R. Lu, X. Zhao, J. Li, P. Niu, B. Yang, H. Wu, W. Wang, H. Song, B. Huang, N. Zhu, Y. Bi, X. Ma, F. Zhan, L. Wang, T. Hu, H. Zhou, Z. Hu, W. Zhou, L. Zhao, J. Chen, Y. Meng, J. Wang, Y. Lin, J. Yuan, Z. Xie, J. Ma, W.J. Liu, D. Wang, W. Xu, E. C. Holmes, G.F. Gao, G. Wu, W. Chen, W. Shi, W. Tan, Genomic characterisation and epidemiology of 2019 novel coronavirus: implications for virus origins and receptor binding, *Lancet* 395 (2020) 565–574.
- [33] Y. Xu, B. Chen, M. He, B. Hu, A homogeneous nucleic acid assay for simultaneous detection of SARS-CoV-2 and influenza A (H3N2) by single-particle inductively coupled plasma mass spectrometry, *Anal. Chim. Acta* 1186 (2021), 339134.
- [34] Z. Li, X. Chen, Z. Huang, J. Zhou, R. Liu, Y. Lv, Multiplex nucleic acid assay of SARS-CoV-2 via a lanthanide nanoparticle-tagging strategy, *Anal. Chem.* 93 (2021) 12714–12722.
- [35] M. Kipping, D. Tanzler, A. Sinz, A rapid and reliable liquid chromatography/mass spectrometry method for SARS-CoV-2 analysis from gargle solutions and saliva, *Anal. Bioanal. Chem.* 413 (2021) 6503–6511.
- [36] N.L. Dollman, J.H. Griffin, K.M. Downard, Detection, mapping, and proteotyping of SARS-CoV-2 coronavirus with high resolution mass spectrometry, *ACS Infect. Dis.* 6 (2020) 3269–3276.
- [37] Y. Peng, Y. Pan, Z. Sun, J. Li, Y. Yi, J. Yang, G. Li, An electrochemical biosensor for sensitive analysis of the SARS-CoV-2 RNA, *Biosens. Bioelectron.* 186 (2021), 113309.
- [38] J. Jiao, C. Duan, L. Xue, Y. Liu, W. Sun, Y. Xiang, DNA nanoscaffold-based SARS-CoV-2 detection for COVID-19 diagnosis, *Biosens. Bioelectron.* 167 (2020), 112479.
- [39] P. Fozouni, S. Son, M. Diaz de Leon Derby, G.J. Knott, C.N. Gray, M.V. D'Ambrosio, C. Zhao, N.A. Switz, G.R. Kumar, S.I. Stephens, D. Boehm, C.L. Tsou, J. Shu, A. Bhuiya, M. Armstrong, A.R. Harris, P.Y. Chen, J.M. Osterloh, A. Meyer-Franke, B. Joehnk, K. Walcott, A. Sil, C. Langelier, K.S. Pollard, E.D. Crawford, A. S. Puschnik, M. Phelps, A. Kistler, J.L. DeRisi, J.A. Doudna, D.A. Fletcher, M. Ott, Amplification-free detection of SARS-CoV-2 with CRISPR-Cas13a and mobile phone microscopy, *Cell* 184 (2021) 323–333, e9.
- [40] G. Qiu, Z. Gai, Y. Tao, J. Schmitt, G.A. Kullak-Ublick, J. Wang, Dual-functional plasmonic photothermal biosensors for highly accurate severe acute respiratory syndrome coronavirus 2 detection, *ACS Nano* 14 (2020) 5268–5277.
- [41] C. Hwang, N. Park, E.S. Kim, M. Kim, S.D. Kim, S. Park, N.Y. Kim, J.H. Kim, Ultrafast and recyclable DNA biosensor for point-of-care detection of SARS-CoV-2 (COVID-19), *Biosens. Bioelectron.* 185 (2021), 113177.
- [42] S.A. Byrnes, R. Gallagher, A. Steadman, C. Bennett, R. Rivera, C. Ortega, S. T. Motley, P. Jain, B.H. Weigl, J.T. Connelly, Multiplexed and extraction-free amplification for simplified SARS-CoV-2 RT-PCR tests, *Anal. Chem.* 93 (2021) 4160–4165.